

# Mass-corrections to double-Higgs production & TopoID

---

**Jonathan Grigo and Jens Hoff<sup>\*†</sup>**

*Institut für Theoretische Teilchenphysik, Karlsruhe Institute of Technology (KIT)*

*E-mail:* jonathan.grigo@kit.edu, jens.hoff@kit.edu

We consider power corrections due to a finite top-quark mass  $M_t$  to the production of a Higgs boson pair within the Standard Model at next-to-leading order (NLO) in QCD. Previous calculations for this process and at this precision were done in the limit of an infinitely heavy top quark. Our results for the inclusive production cross section at NLO include terms up to  $\mathcal{O}(1/M_t^{12})$ .

We present the *Mathematica* package *TopoID* which for arbitrary processes aims to perform the necessary steps from Feynman diagrams to unrenormalized results expressed in terms of master integrals. We employ it for advancing in this process towards next-to-next-to-leading order (NNLO) where further automatization is needed.

*Loops and Legs in Quantum Field Theory*

*27 April 2014 - 02 May 2014*

*Weimar, Germany*

---

<sup>\*</sup>Speaker.

<sup>†</sup>This work was supported by the DFG through the SFB/TR9 “Computational Particle Physics” and the Karlsruhe School of Elementary Particle and Astroparticle Physics (KSETA). We would like to thank Kirill Melnikov and Matthias Steinhauser for the productive collaboration and also for numerous cross-checks and useful suggestions concerning *TopoID*.

## 1. Introduction

It is still an open question whether the scalar particle discovered by ATLAS and CMS [1, 2] at CERN is indeed the Higgs boson of the Standard Model (SM). In forthcoming years its couplings to the various gauge bosons and fermions will be measured with improved precision to verify their compatibility with the values dictated within the SM. But to gain insight into the mechanism of electroweak symmetry breaking the particles self-interactions need to be probed, too. The process granting this possibility is production of a Higgs boson pair via gluon fusion which has two contributions: One where both Higgs bosons couple to top quarks, the other one involves the cubic coupling  $\lambda$  of the SM Higgs potential (see fig. 3)

$$V(H) = \frac{1}{2}m_H^2 H^2 + \lambda v H^3 + \frac{1}{4}\lambda H^4, \quad (1.1)$$

with the Higgs mass  $m_H$ , vacuum expectation value  $v$ , and  $\lambda = m_H^2/2v^2 \approx 0.13$  for the SM. Note that the influence of the second contribution is strongly suppressed compared to the first one, but becomes noticeable through its large destructive interference. The process has a relatively small cross section and suffers from large backgrounds, making the extraction of the Higgs self-interaction at the LHC a challenge. However, a number of studies suggest the prospect of measuring  $\lambda$  [4, 3, 5, 6], some within an accuracy of about 30% with at least  $3000 \text{ fb}^{-1}$  accumulated luminosity [5, 6].

The leading order (LO) result with exact dependence on the top quark mass  $M_t$  has been known since long [7, 8]. Further terms in the perturbation series have been computed in the approximation of an infinitely heavy top quark  $M_t \rightarrow \infty$  at NLO [9] and just recently at NNLO [10]. It is important to remark that doing so, the exact LO result has been factored off in the NLO and NNLO contributions.

## 2. Results

It is known that the  $1/M_t$  expansion works extremely well for the case of a single Higgs boson [11, 12, 13] employing the aforesaid factorization procedure. For that reason we computed for double-Higgs production at NLO power corrections due to a finite top quark mass to the total cross section in the following way:

$$\sigma_{\text{expanded}}^{\text{NLO}} \rightarrow \sigma_{\text{exact}}^{\text{LO}} \frac{\sigma_{\text{expanded}}^{\text{NLO}}}{\sigma_{\text{expanded}}^{\text{LO}}}, \quad (2.1)$$

where numerator and denominator are expanded to the same order in  $1/M_t$ . In [14] we presented results expanded up to  $\mathcal{O}(1/M_t^8)$  and in [15] to  $\mathcal{O}(1/M_t^{10})$ , here they are available to  $\mathcal{O}(1/M_t^{12})$ . The discussion of results has not changed by including the new terms. Therefore we only want to show updated plots for the hadronic cross section, see fig. 1 and fig. 2 and summarize our findings.

- The common enhancement by gluon luminosity of low- $\hat{s}$  contributions, for which we observe good convergence, enlarges the validity range of the expansion.
- Including  $1/M_t$  corrections is necessary to detect deviations in  $\lambda$  of  $\mathcal{O}(10\%)$ .

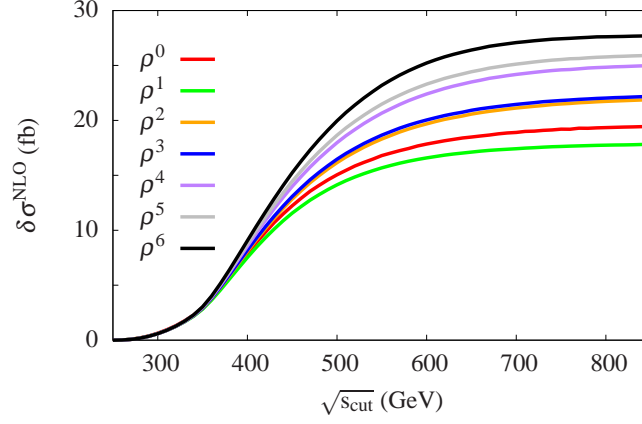


**Figure 1:** NLO contribution (without LO) to the hadronic cross section. The color coding indicates higher expansion orders in  $\rho = m_H^2/M_t^2$ .  $\sqrt{s_{\text{cut}}}$ , a cut on the partonic  $\hat{s}$ , can be seen as an approximation for the invariant mass of the Higgs pair.

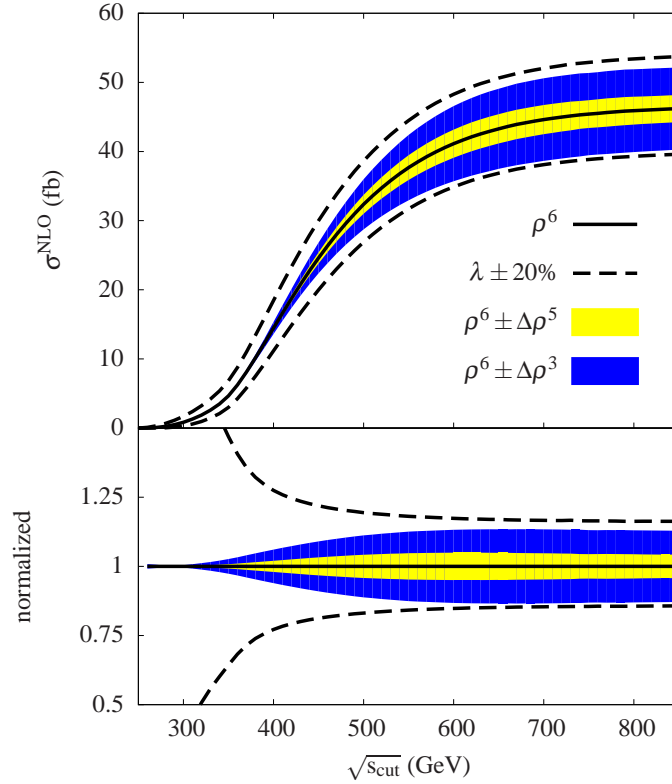


**Figure 2:** The straight black line shows the hadronic NLO cross section up to  $\mathcal{O}(\rho^6)$ , the dashed black lines indicate the variation from changing the SM value of  $\lambda$  within  $\pm 20\%$ . The yellow and the blue band show the theoretical uncertainty by taking the difference to the  $\mathcal{O}(\rho^5)$  and to the  $\mathcal{O}(\rho^3)$  expansion, respectively.

$$\sigma_{\text{tot.}}(gg \rightarrow HH) \sim \text{Disc.}(\mathcal{M}(gg \rightarrow gg))$$

$$\int d\text{PS} \left| \begin{array}{c} \text{[Diagram 1: Box with top quarks]} \\ + \text{[Diagram 2: Triangle with top quarks]} \end{array} \right|^2 \sim$$

$$\begin{array}{c} \text{[Diagram 3: Two boxes]} \\ + \text{[Diagram 4: Box and triangle]} \\ + \text{[Diagram 5: Two triangles]} \end{array}$$

**Figure 3:** For Higgs boson pair production we only need to consider cuts (denoted by short dashed vertical lines) through two Higgs bosons (long dashed black lines) and additional partons (beginning at NLO). This correspondence is depicted here for the LO order contributions. Curly red lines represent gluons, straight blue lines massive top quarks.

- Compared to the prediction in the  $M_t \rightarrow \infty$  limit we obtain for the LHC at 14 TeV

$$\begin{aligned} \sigma^{\text{NLO}}(pp \rightarrow HH) &= 19.7^{\text{LO}} + 19.0^{\text{NLO}, M_t \rightarrow \infty} \text{ fb} \\ \rightarrow \sigma^{\text{NLO}}(pp \rightarrow HH) &= 19.7^{\text{LO}} + (27.3 \pm 5.9)^{\text{NLO}, 1/M_t^{12}} \text{ fb}, \end{aligned} \quad (2.2)$$

where no cut on the partonic center-of-mass energy  $\hat{s}$  was applied and equal factorization and renormalization scale  $\mu = 2m_H$  was chosen.

- This can be either seen as an improvement of current precision with corrections of about 20% or at least as reliable error estimate for a NLO computation of this process.

### 3. Techniques

Being interested mainly in the total cross section  $gg \rightarrow HH$ , we can make use of the optical theorem (see, e.g., [16]) and compute imaginary parts or discontinuities of the amplitude  $\mathcal{M}(gg \rightarrow gg)$  related to a Higgs pair instead of squaring  $\mathcal{M}(gg \rightarrow HH)$  and performing the phase space integration (see fig. 3). On the one hand this method simplifies the calculation, namely: forward scattering kinematics, common treatment of contributions related to different phase space integrations and computation of the latter only in the very end at master integral level. On the other hand, one has to compute a larger number of diagrams with more loops.

The second ingredient making this calculation feasible is the asymptotic expansion at diagrammatic level (see, e.g., [17]) in the hierarchy  $M_t^2 \gg \hat{s}, m_H^2$  which corresponds to a series expansion of an analytic result in the parameter  $\rho = m_H^2/M_t^2$ . This procedure effectively reduces the number of loops and scales in the integrals to be evaluated (see fig. 4), thus diminishing some of the drawbacks connected to use of the optical theorem.

Within this framework our toolchain for the various steps of the calculation looks as follows:

1. generation of Feynman diagrams with QGRAF [18],
2. selection of diagrams which have the correct cuts [19],
3. asymptotic expansion with q2e and exp [20, 21],

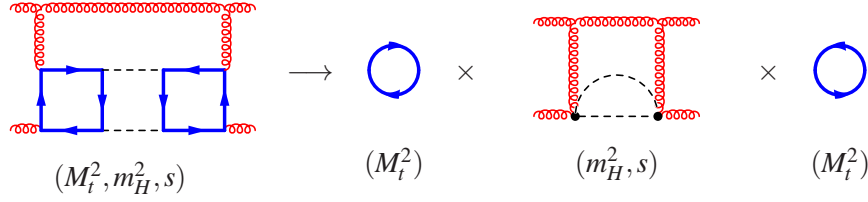


**Figure 4:** Applying the rules for asymptotic expansion to a single Feynman diagram one obtains in general a sum of contributions (there is only one in this example). Each contribution in turn is a product of subgraphs (containing the hard scale;  $M_t^2$  in our case) and co-subgraphs (containing the soft scales;  $m_H^2, s$ ). The notation is as in fig. 3.

4. reduction to scalar integrals in FORM [22, 23] and/or TFORM [24],
5. reduction to master integrals by rows [19] and/or FIRE [25, 26],
6. minimization of the set of master integrals [19].

Step 2 is necessary since one cannot steer QGRAF in such a way that only diagrams with a specific cut structure are generated. Because of that we filter the diagrams provided by QGRAF for those which exhibit an appropriate cut in the  $s$ -channel corresponding to an interference term from squaring the amplitude for  $gg \rightarrow HH$ . (Usually only about 10-30% of the initial diagrams pass the filter.) At NLO step 4 turned out to be the bottleneck of the calculation for going to higher orders in the expansion parameter  $\rho$ .

#### 4. TopoID

Up to now the input for steps 3-6 in the above list was usually provided manually. For going beyond NLO we use TopoID to provide all that information in an automatic fashion. More precisely: all the graphs corresponding to a topology as “mapping patterns” for step 3, FORM code processing aforementioned topologies in step 4 and definitions of topologies suitable for reduction with the programs listed for step 5.

When performing a multi-loop calculation one often works with a set of topologies and within each topology integrals are reduced to a finite set of master integrals. The same master integral may thus be represented in different ways by single integrals of various topologies. TopoID is capable of providing such an identification, as are recent versions of FIRE [26]. Moreover, there exist also non-trivial *linear* relations involving multiple “master integrals” which can be found with the help of this package (step 6).

A diagram class or family  $T$ , usually referred to as topology, is a set of  $N$  scalar propagators  $\{d_i\}$  with arbitrary powers  $\{a_i\}$ , usually referred to as indices, composed of masses  $\{m_i\}$  and line momenta  $\{q_i\}$ . The line momenta  $\{q_i\}$  are linear combinations of  $E$  external momenta  $\{p_i\}$  and  $I$

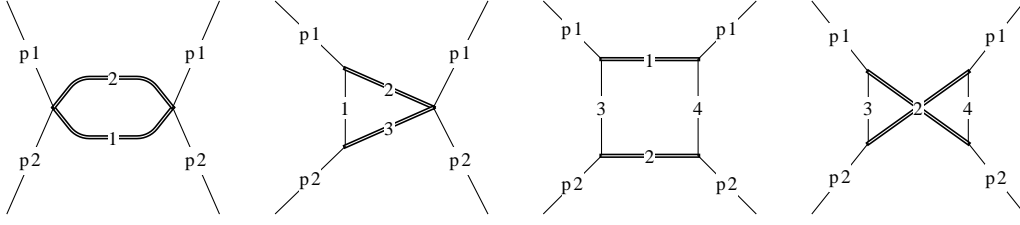


**Figure 5:** Sample one-loop topologies appearing after asymptotic expansion at LO, NLO and NNLO (the last two). The first graph is an example of a linearly independent, but incomplete topology. The second topology is a linearly independent and complete. The last two topologies, one planar, one non-planar, are linearly dependent and complete. Plain black lines are massless, the double lines carry the Higgs mass.

internal momenta  $\{k_i\}$  with integers  $c_{ij}, d_{ij}$ ,

$$T(a_1, \dots, a_N) = \left\{ \prod_{i=1}^I \int dk_i^D \right\} \left\{ \prod_{j=1}^N \frac{1}{[m_j^2 + q_j^2]^{a_j}} \right\}, \quad (4.1)$$

$$q_i = \sum_{j=1}^E c_{ij} p_j + \sum_{j=1}^I d_{ij} k_j. \quad (4.2)$$

For particular kinematics, i.e. given external and internal momenta, supplemented by possible constraints, e.g. putting particles on-shell, one can form all occuring scalar products

$$x_{p_i p_j} = p_i \cdot p_j, \quad s_{p_i p_j} = p_i \cdot p_k, \quad s_{k_i k_j} = k_i \cdot k_j. \quad (4.3)$$

If the denominators of a topology  $\{d_i\}$  allow for expressing each of the internal scalar products  $s_{ij}$  the topology is complete, otherwise incomplete. In the latter case affected scalar products are called irreducible scalar products and appear only as numerators (fig. 5 shows some examples for Higgs pair production).

Diagram topologies, i.e. mapping patterns for Feynman diagrams, in general are incomplete and also linearly dependent, viz. linear relations among the  $\{d_i\}$  exist. In contrast, reduction topologies need to be linearly independent and complete. This is exemplified in fig. 6 with the two-loop topologies emerging after asymptotic expansion of the purely virtual five-loop diagrams at NNLO<sup>1</sup>. The mapping between these two types of topologies can in general become quite intricate for larger sets but is handled easily by TopoID.

The foundation of this automatization is the  $\alpha$ -representation of Feynman integrals

$$T(a_1, \dots, a_N) = c \left\{ \prod_{i=1}^N \int_0^\infty d\alpha_i \right\} \delta(1 - \sum_{i=1}^N \alpha_i) \left\{ \prod_{j=1}^N \alpha_j^{a_j} \right\} \mathcal{U}^a \mathcal{W}^b, \quad (4.4)$$

where  $c, a$  and  $b$  depend on  $I, D$  and the  $\{a_i\}$  only. The polynomials  $\mathcal{U}$  and  $\mathcal{W}$  are homogeneous in the  $\{\alpha_i\}$  and encode the complete information on the topology (for further details see, e.g., ref. [27]). This representation is unique up to renaming of the  $\alpha$ -parameters, but this ambiguity

<sup>1</sup>In this case two massive tadpole diagrams containing the top quarks (one with one loop and one with two loops) and a two-loop box diagram with Higgs mass remain after asymptotic expansion.

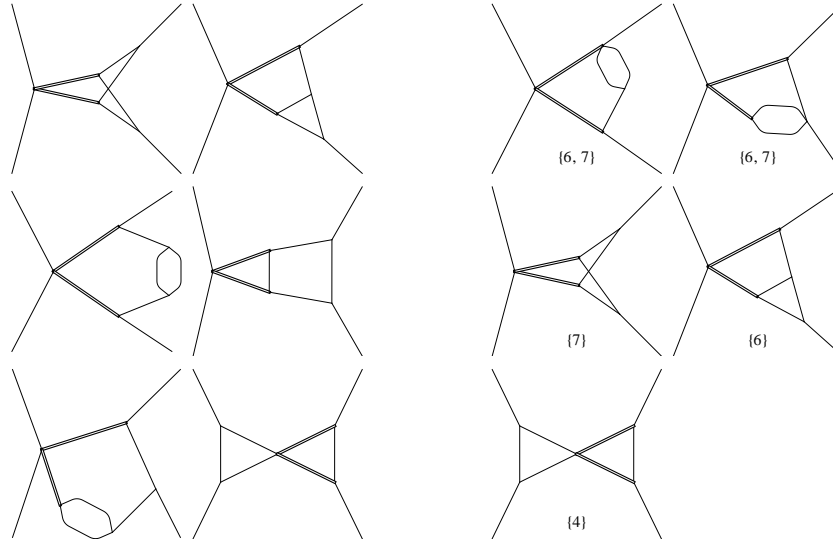


**Figure 6:** The left hand side shows the set of diagram topologies, the right hand side the set of reduction topologies. Their order is chosen by TopoID in a fixed way, numbers in braces denote the presence of irreducible numerators. The last topology in both sets is an example of a factorizing topology. Note the modification of self-energy insertions from the left to the right side, propagators carrying the same momentum are identified. Furthermore, there is a non-trivial mapping from the second and fourth diagram topology to the fourth reduction topology which cannot be deduced from the graphs alone.

can be eliminated by applying the procedure described in [28] to derive a canonical form of the  $\alpha$ -representation, making it a suitable identifier.

TopoID is a generic, process independent tool and bridges the gap between Feynman diagrams and unrenormalized results expressed in terms of *actual* master integrals, i.e. including the non-trivial relations, in a completely automatic way. It is written as a package for Mathematica which offers a high-level programming environment and the demanded algebraic capabilities. However, for the actual calculation FORM code is generated to process the diagrams in an effective way. Let us briefly summarize features the package has to offer:

- topology identification and construction of a minimal set of topologies,
- classification of distinct and scaleless subtopologies,
- access to properties such as completeness, linear dependence, etc.,
- construction of partial fractioning relations,
- revealing symmetries (completely within all levels of subtopologies),
- graph manipulation, treatment of unitarity cuts, factorizing topologies,
- FORM code generation (diagram mapping, topology processing, Laporta reduction),
- master integral identification (arbitrary base changes, non-trivial relations).

As one cross-check we repeated the NLO calculation within this automatized setup and found agreement with our previous calculation.

## References

- [1] G. Aad *et al.* [ATLAS Collaboration], Phys. Lett. B **716** (2012) 1 [arXiv:1207.7214 [hep-ex]].
- [2] S. Chatrchyan *et al.* [CMS Collaboration], Phys. Lett. B **716** (2012) 30 [arXiv:1207.7235 [hep-ex]].
- [3] U. Baur, T. Plehn and D. L. Rainwater, Phys. Rev. D **69** (2004) 053004 [hep-ph/0310056].
- [4] J. Baglio, A. Djouadi, R. Gröber, M. M. Mühlleitner, J. Quevillon and M. Spira, JHEP **1304** (2013) 151 [arXiv:1212.5581 [hep-ph]].
- [5] F. Goertz, A. Papaefstathiou, L. L. Yang and J. Zurita, JHEP **1306** (2013) 016 [arXiv:1301.3492 [hep-ph]].
- [6] V. Barger, L. L. Everett, C. B. Jackson and G. Shaughnessy, Phys. Lett. B **728** (2014) 433 [arXiv:1311.2931 [hep-ph]].
- [7] E. W. N. Glover and J. J. van der Bij, Nucl. Phys. B **309** (1988) 282.
- [8] T. Plehn, M. Spira and P. M. Zerwas, Nucl. Phys. B **479** (1996) 46 [Erratum-ibid. B **531** (1998) 655] [hep-ph/9603205].
- [9] S. Dawson, S. Dittmaier and M. Spira, Phys. Rev. D **58** (1998) 115012 [hep-ph/9805244].
- [10] D. de Florian and J. Mazzitelli, Phys. Rev. Lett. **111** (2013) 201801 [arXiv:1309.6594 [hep-ph]].
- [11] A. Pak, M. Rogal and M. Steinhauser, JHEP **1002** (2010) 025 [arXiv:0911.4662 [hep-ph]].
- [12] S. Marzani, R. D. Ball, V. Del Duca, S. Forte and A. Vicini, Nucl. Phys. B **800** (2008) 127 [arXiv:0801.2544 [hep-ph]].
- [13] R. V. Harlander and K. J. Ozeren, JHEP **0911** (2009) 088 [arXiv:0909.3420 [hep-ph]].
- [14] J. Grigo, J. Hoff, K. Melnikov and M. Steinhauser, Nucl. Phys. B **875** (2013) 1 [arXiv:1305.7340 [hep-ph]].
- [15] J. Grigo, J. Hoff, K. Melnikov and M. Steinhauser, PoS RADCOR **2013** (2014) 006 [arXiv:1311.7425 [hep-ph]].
- [16] C. Anastasiou and K. Melnikov, Nucl. Phys. B **646** (2002) 220 [hep-ph/0207004].
- [17] V. A. Smirnov, Springer Tracts Mod. Phys. **177** (2002) 1.
- [18] P. Nogueira, J. Comput. Phys. **105** (1993) 279.
- [19] J. Hoff, A. Pak, (unpublished).
- [20] R. Harlander, T. Seidensticker and M. Steinhauser, Phys. Lett. B **426** (1998) 125 [hep-ph/9712228].
- [21] T. Seidensticker, hep-ph/9905298.
- [22] J. A. M. Vermaseren, math-ph/0010025.
- [23] J. Kuipers, T. Ueda, J. A. M. Vermaseren and J. Vollinga, Comput. Phys. Commun. **184** (2013) 1453 [arXiv:1203.6543 [cs.SC]].
- [24] M. Tentyukov and J. A. M. Vermaseren, Comput. Phys. Commun. **181** (2010) 1419 [hep-ph/0702279 [HEP-PH]].
- [25] A. V. Smirnov, JHEP **0810** (2008) 107 [arXiv:0807.3243 [hep-ph]].
- [26] A. V. Smirnov and V. A. Smirnov, Comput. Phys. Commun. **184** (2013) 2820 [arXiv:1302.5885 [hep-ph]].
- [27] V. A. Smirnov, Springer Tracts Mod. Phys. **250** (2012) 1.
- [28] A. Pak, J. Phys. Conf. Ser. **368** (2012) 012049 [arXiv:1111.0868 [hep-ph]].